1,1-Bis(4-hydroxyphenyl)-2-ferrocenylbutane

Jérémy Forté, Patrick Herson, Pascal Pigeon

molbank

MDPI

Short Note

1,1-Bis(4-hydroxyphenyl)-2-ferrocenylbutane

Jérémy Forté [1], Patrick Herson [1,†] and Pascal Pigeon [1,2,*]

[1] CNRS, Institut Parisien de Chimie Moléculaire (IPCM), Sorbonne Université, 4 Place Jussieu, 75005 Paris, France; jeremy.forte@sorbonne-universite.fr (J.F.)
[2] PSL, Chimie ParisTech, 11 Rue Pierre et Marie Curie, 75005 Paris, France
* Correspondence: pascal.pigeon@chimieparistech.psl.eu or pascal.pigeon@sorbonne-universite.fr
† P. Herson passed away in October 2017. Patrick Herson worked at Sorbonne University from 1974 to 2016. First involved in synthetic chemistry he progressively shifted his interest to crystal structure analysis and became a key figure of the X-ray Diffraction facility. During his career, he solved hundreds of crystal structures, particularly in the field of molecular chemistry.

Abstract: Ferrociphenols are anticancer organometallic molecules bearing a ferrocene group linked, at least, to one *para*-phenol moiety via a double bond. Up to the present, their biological activity has been thought to be linked to their oxidation within cells to form a reactive quinone-methide metabolite with the participation of this central double bond. To prove this assertion, the alkenyl entity of ferrociphenol **1a** (1,1-bis-(4-hydroxyphenyl)-2-ferrocenylbut-1-ene) was reduced by triethylsilane in an acidic medium to obtain the alkyl counterpart 1,1-bis(4-hydrophenyl)-2-ferrocenylbutane. 1,1-bis(4-hydrophenyl)-2-ferrocenylbutane was fully characterized by ^{1}H NMR (including COSY), ^{13}C NMR, HRMS, IR, elemental analysis and X-ray diffraction (XRD). Although missing the central double bond, this compound remains biologically active, opening the way to a new family of anticancer ferrocene-containing molecules.

Keywords: ferrocene; ferrociphenol; alkene reduction; anticancer molecules; organometallic compounds; X-ray diffraction; crystal structure

Citation: Forté, J.; Herson, P.; Pigeon, P. 1,1-Bis(4-hydroxyphenyl)-2-ferrocenylbutane. *Molbank* **2024**, *2024*, M1932. https://doi.org/10.3390/M1932

Academic Editor: Nicholas Leadbeater

Received: 17 November 2024
Revised: 1 December 2024
Accepted: 4 December 2024
Published: 6 December 2024

1. Introduction

In the fight against cancer, the interest in organometallic complexes, particularly ferrocene-containing molecules, has increased significantly over the last two decades [1–12]. Within this family of molecules, ferrociphenols show high cytotoxic activity against various cancer cell lines. Initially, one of the three phenyl groups of Tamoxifen, a selective estrogen receptor modulator (SERM) used in the adjuvant treatment of hormone-dependent breast cancer, was replaced by a ferrocenyl group to form a new compound called Ferrocifen, by analogy to Tamoxifen. Ferrociphenol **1a** (Figure 1) is a precursor in the synthesis of 4-Hydroxyferrocifen **1b**, i.e., the ferrocenyl version of 4-hydroxytamoxifen, the active metabolite of Tamoxifen. Compound **1b** showed antiproliferative activity against the hormone-dependent human breast cancer MCF-7 cell line as well as against the triple-negative MDA-MB-231 cell line. By serendipity, we found that precursor **1a** was also very active against both the MDA-MB-231 and MCF-7 cell lines [13]. The cytotoxic activity of **1a** and **1b** is associated with the [ferrocene-alkene-*p*-phenol] moiety that participates in metabolite formation by oxidation (see below) [14]. In the twenty years following these discoveries, we synthesized many ferrociphenols, sometimes with great variation in structure—for instance, the cyclic version of **1a** (ferrocenophane **2**) or the replacement of a phenyl group by an alkyl group (ferrocenyl derivatives of diethylstilbestrol **3a–d**)—all sharing the central double bond linking the ferrocenyl and aryl groups and being active to very active. For example, the IC_{50}s of the acyclic compounds **1a** [13], **1b**, **1c** [15], **1d** [16], **3a**, **3b**, **3c** and **3d** acting on MDA-MB-231 cells are 0.64, 0.5, 0.11, 0.035, 1.14, 0.14, 0.28 and 0.36 µM, respectively. Ferrocenophane **2** has an IC_{50} of 0.089 µM. This systematic activity was attributed to oxidation within cells, yielding a quinone methide able to covalently bind

to proteins [17]. The formation of quinone methide proceeds via a multistep mechanism involving two one-electron oxidation steps and two deprotonation steps [6].

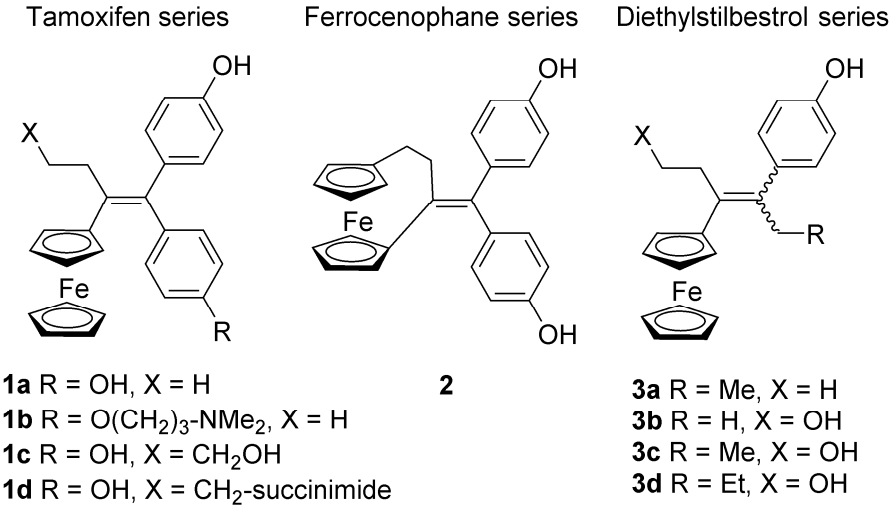

Figure 1. Examples of the diversity of the ferrociphenol family, including the Tamoxifen-like family **1**, the cyclic ferrocenophane derivative **2** and the diethylstilbestrol-like derivatives **3**.

We wondered whether a disconnection between the ferrocenyl group and the phenol group would have any effect on the biological activity of ferrociphenol **1a**. Thus, we decided to reduce its double bond by chemical hydrogenation using triethylsilane and trifluoroacetic acid (TFA). As a great simplification, TFA brings H^+ and triethylsilane brings H^-. We have already used this method to reduce carbocations generated by TFA from an alcohol, from an alkene or even directly from a ketone. The reduced compound **4** was obtained from **1a** in moderate yield (60%) after three days of reaction at room temperature in dichloromethane in the presence of TFA and $HSiEt_3$. Surprisingly, compound **4** was still cytotoxic to MDA-MB-231 cells, with an IC_{50} that only doubled (IC_{50} = 0.94 ± 0.11 μM) with respect to **1a** (IC_{50} = 0.64 ± 0.06 μM). This opens up possibilities for the widening of the diversity of active ferrocenyl compounds, starting with reduced versions of our most active compounds, i.e., **1b–d** and **2**. As the first and leading molecule of this new family, **4** was fully characterized by ^{1}H NMR, ^{13}C NMR, COSY, IR, elemental analysis and X-ray diffraction (XRD).

2. Results and Discussion

2.1. Synthesis of **4**

Compound **4** was synthesized from compound **1a** by reduction with triethylsilane and trifluoroacetic acid (TFA) in a dichloromethane solution at room temperature for three days, with a yield of 60% (Scheme 1). Recrystallization from dichloromethane provided crystals suitable for X-ray diffraction analysis. Compared to that of **1a**, the ^{1}H NMR spectrum of **4** (Supplementary Figures S1 and S2) shows the appearance of signals assigned to the two new protons in positions 1 and 2 of the butane skeleton, namely, a doublet for H1 partially hidden by the signal of the ferrocene protons (Figure S1) at 3.99 ppm and a multiplet for H2 at 3.15 ppm. Both protons were coupled together, as shown by the COSY experiment (Figure S2). Anisotropy due to the generation of a stereogenic center also made the protons of the methylene (H3) and ferrocenyl (C_5H_4) groups inequivalent. These two methylene protons, H3, were coupled with H2 and not H1 (Figure S2), confirming this attribute. In the ^{13}C NMR spectrum, two quaternary carbon atoms disappeared and were replaced by two CH groups (C1 and C2) at 55.1 and 46.0 ppm, respectively (Figures S3 and S4).

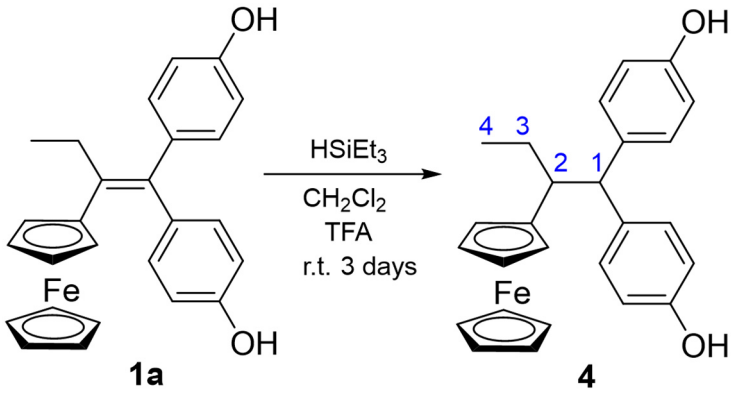

Scheme 1. Reduction of alkene **1a** into alkane **4**. Systematic numbering (IUPAC) of the butane skeleton.

2.2. X-Ray Crystal Structure Determination

The crystal structure of **4** was determined by X-ray diffraction (XRD) (Figure 2). Orange crystals were obtained and grown by the slow evaporation of a CH_2Cl_2 solution under ambient conditions. Under these conditions, compound **4** crystallized in the $P\bar{1}$ space group (triclinic system). The asymmetric unit contains one molecule of **4** and a half-molecule of CH_2Cl_2. Crystallographic and refinement structure data are available in Table 1.

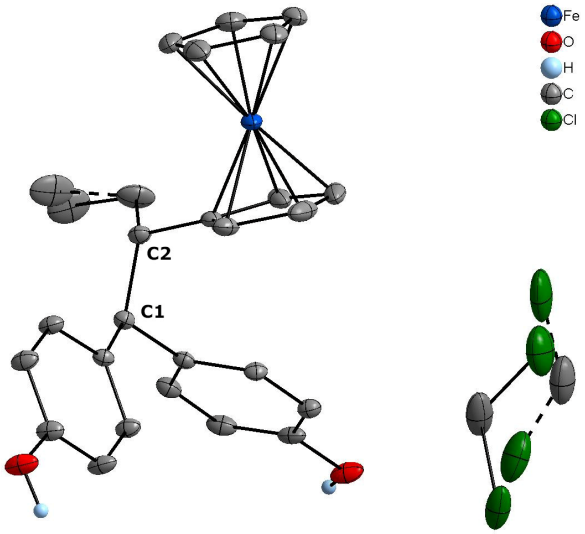

Figure 2. Crystal structure of **4**, co-crystallized with a disordered half dichloromethane molecule (CCDC 2393186). Ellipsoids are drawn with 30% probability. Almost all hydrogen atoms are omitted for the sake of clarity. Only H atoms involved in H-bonds are shown. Black dotted lines are bonds between atoms occupying minor positions. C1–C2 bond length at 200 K: 1.580(2) Å.

Dichloromethane is disordered over two positions with an occupation rate of 42/8. The presence of a partial CH_2Cl_2 molecule in the asymmetric unit is confirmed by elemental analysis. The proportions of CH_2Cl_2 determined by XRD and elemental analysis are different (0.50 vs. 0.25 of a molecule of dichloromethane per molecule of **4**, respectively). This difference is probably due to the vaporization of CH_2Cl_2 and the two analyses being performed at different temperatures and times. It is also interesting to note the presence of CH_2Cl_2 in the ^{1}H NMR results (Figure S1). Therefore, the presence of partial CH_2Cl_2 is only proved qualitatively.

Regarding **4**, the C1-C2 bond length is 1.58 Å, corresponding to a simple bond. This result proves the reduction of the double bond of **1a**. For comparison, the bond in **1a** has a length of 1.38Å (see CCDC 739363 [18]). The ethyl group bound to C1 is disordered between two very close positions with an occupancy rate of 60/40. Each phenol group is involved in

hydrogen bonds. One is connected to the second phenol group of the neighboring molecule obtained by b-axis translation. The other is connected to the first phenol group of the neighboring molecule obtained using an inversion center, located under the two phenol groups of the first molecule. The network created by these H-bonds resembles an almost perfect square ($O_i \ldots O_j \ldots O_i$ angles: 94.3 and 85.7°; distortion angle: 0°; Figure 3). H-bond lengths and angles are available in Table 2.

Table 1. Crystallographic and refinement structure data for **4**.

Parameter	Value	Parameter	Value
CCDC deposit number	2393186	Crystal size (mm²)	0.23 × 0.16 × 0.14
Empirical formula [a]	$C_{26.5}H_{27}ClFeO_2$	Wavelength λ (Å)	0.71073
Moiety Formula	$C_{26}H_{26}FeO_2$, 0.5 (CH_2Cl_2)	2θ range (°)	3.646–59.998
Formula weight (g/mol)	468.78	Miller indices ranges	$-11 \leq h \leq 11$, $-16 \leq k \leq 16$, $-17 \leq l \leq 15$
Temperature (K)	200		
Crystal system	Triclinic		
Space group	$P\bar{1}$	Measured reflections	20976
a (Å)	8.4426 (9)	Unique reflections	6734
b (Å)	11.6967 (14)	R_{int}/R_{sigma}	0.0275/0.0312
c (Å)	12.4258 (10)	Reflections [$I \geq 2\sigma(I)$]	5273
α (°)	78.249 (7)	Restraints	77
β (°)	83.969 (7)	Parameters	336
γ (°)	76.411 (11)	Goodness of fit F²	1.032
Volume (Å^3)	1165.6 (2)	Final R indices [bc] [all data]	R1 = 0.0606, wR2 = 0.1093
Z	2		
ρ_{calc} (g/cm^3)	1.336	Final R indices [bc] [$I \geq 2\sigma(I)$]	R1 = 0.0411, wR2 = 0.0973
Absorption coefficient μ (mm^{-1})	0.782 (MoKα)		
F(000)	490	Largest diff. peak/hole (e/Å3)	0.54/−0.63

[a] Including solvent molecules (if present); [b] $R1 = \sum||F_o| - |F_c||/\sum|F_o|$; [c] $wR2 = \sqrt{\sum(w(F_o^2 - F_c^2))/\sum\left(w(F_o^2)^2\right)}$.

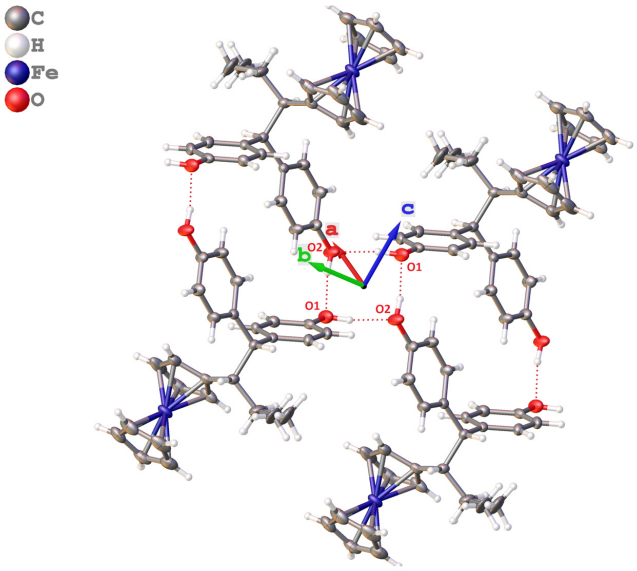

Figure 3. Network of hydrogen bonds in the crystal structure of **4**. H-bonds are shown by red dotted lines. Ellipsoids are drawn with 50% probability. Dichloromethane is omitted for simplicity. Axes of cell are depicted in red (a), green (b) and blue (c) arrows. O1-O2-O1 and O2-O1-O2 angles at 200 K: 94.316(62)° and 85.684(63)°. O1-O2-O1-O2 distortion angle at 200 K: 0.000(63)°.

Table 2. H-bond lengths and angles in the crystal structure of **4** at 200 K.

D-H…A	D-H (Å)	H…A (Å)	D…A (Å)	D-H…A (°)
O1-H1….O2 [i]	0.94(2)	1.85(2)	2.758(2)	161(2)
O2-H2…O1 [ii]	0.92(3)	1.88(3)	2.788(2)	170(2)

D—H-donor atom; H—hydrogen atom; A—H-acceptor atom. Symmetry codes: (i) x, −1 + y, z; (ii) 2 − x, 1 − y, 2 − z.

3. Materials and Methods

3.1. General Procedure

^{1}H and ^{13}C-NMR spectra were acquired using Bruker 300 and 400 MHz spectrometers (Bruker France, 67166 Wissembourg, France, bs = broad singlet; d = doublet; t = triplet; m = multiplet). EI-MS was performed using a Nermag R 10-10C spectrometer; ESI-MS using a triple quadrupole mass spectrometer API 3000 LC–MS/MS system (Applied Biosystems, Sciex, Framingham, MA 01701, USA) in positive-ion mode; and high-resolution mass spectrometry (HRMS) using a Jeol MS 7000 instrument (JEOL Europe SAS, 78290 Croissy-sur-Seine, France). IR spectra were recorded on an FT-IR spectrometer (Tensor 27, Bruker France, 67166 Wissembourg, France) equipped with an ATR MIRacle (Pike Technologies inc., Madison WI 53719, USA) accessory. Elemental analyses were performed at the microanalysis laboratory of the CNRS (91190 Gif sur Yvette, France). HPLC purification was conducted on a reverse-phase semi-preparative Kromasil C18 column (402 58 Göteborg, Sweden). Thin-layer chromatography was performed on silica gel 60 GF254 (Merck KGaA, Darmstadt, 64293, Germany). Column chromatography was performed on silica gel 60 M (Merck KGaA, Darmstadt, 64293, Germany). Reagents were obtained from Sigma Aldrich (38297 Saint-Quentin-Fallavier Cedex) and used as received.

*3.2. Synthesis of 1,1-Bis(4-hydroxyphenyl)-2-ferrocenylbutane (**4**)*

Ferrociphenol **1** (0.85 g; 2 mmol; M = 424.31; 1 equiv.) was dissolved in 50 mL of dichloromethane. Triethylsilane (0.96 mL; 6 mmol; M = 116.28; d = 0.728; 3 equiv.) and trifluoroacetic acid (2.07 mL; 26.9 mmol; M = 114.02; d = 1.535; 13.5 equiv.) were added to the solution. The mixture was stirred continuously for three days. Then, it was poured into a saturated bicarbonate solution and extracted twice with dichloromethane. The organic layers were combined, washed with water and dried over magnesium sulfate. After concentration under reduced pressure, the crude product was chromatographed on a silica gel column with cyclohexane/ethyl acetate (1:1) as an eluent. The second fraction, obtained as a red oil, corresponded to the desired product. It was further purified by reverse-phase semi-preparative HPLC using acetonitrile/water (4:1) as an eluent to fully remove excess triethylsilane. Compound **4** (0.51 g; 1.19 mmol; M = 426.33; yield = 60%) was obtained as an orange oil that was successfully recrystallized from dichloromethane for X-ray structure determination.

^{1}H NMR (300 MHz; acetone-d_6): δ = 1.02 (t, J = 7.4 Hz, 3H; CH_3: H4); 1.49–1.67 (m, 1H; CH_2: H3), 1.83–2.02 (m, 1H; CH_2: H3), 3.10–3.21 (m, 1H, C*H*-Et: H2), 3.52 (bs, 1H, CH; C_5H_4), 3.89 (bs, 1H, CH; C_5H_4), 3.99 (d, J = 7.6 Hz, 1H, C*H*-Ar_2: H1), 4.05 (bs, 2H; 2xCH C_5H_4), 4.06 (s, 5H; Cp), 6.64 (d, J = 8.7 Hz, 2H; C_6H_4), 6.73 (d, J = 8.7 Hz, 2H; C_6H_4), 6.93 (d, J = 8.7 Hz, 2H; C_6H_4), 7.09 (d, J = 8.7 Hz, 2H; C_6H_4), 8.04 (bs, 1H; OH), 8.09 (bs, 1H; OH). ^{13}C NMR (75 MHz; acetone-d_6): δ = 12.6 (CH_3), 26.8 (CH_2), 46.0 (CH), 55.1 (CH), 67.2 (2CH; C_5H_4), 68.7 (CH; C_5H_4), 69.4 (5CH; Cp), 70.4 (CH; C_5H_4), 94.0 (C; C_5H_4), 115.3 (2xCH; C_6H_4), 115.6 (2xCH; C_6H_4), 130.4 (2xCH; C_6H_4), 131.2 (2xCH; C_6H_4), 134.8 (C), 136.7 (C), 156.2 (C-OH), 156.3 (C-OH). IR (ATR, ν cm^{-1}): 3472. MS (EI, 70 eV): m/z = 426 $[M]^{+\cdot}$, 227 [ferrocene-CH-Et]$^{+}$, 199 $[(HOC_6H_4)_2CH]^{+}$, 121 $[FeCp]^{+}$. HRMS (EI, 70 eV, $C_{26}H_{26}FeO_2$, $[M]^{+\cdot}$) calcd: 426.1283, found: 426.1284. Anal. Calcd for $C_{26}H_{26}FeO_2(CH_2Cl_2)_{1/4}$: C, 70.44; H, 5.96. Found: C, 70.24; H, 6.17.

3.3. X-Ray Diffraction Experiment

A single crystal of **4** was selected, mounted and transferred into a cold nitrogen gas stream. Intensity data were collected with a Nonius KappaCCD diffractometer using graphite-monochromated MoKα radiation. Data collection, unit-cell parameter determination, integration and data reduction were performed with the Nonius KappaCCD suite of programs [19–21]. The structure was solved with SHELXT [22], and non-hydrogen atoms were refined anisotropically by full-matrix least-squares methods with SHELXL [23] using Olex2 [24]. The structure was deposited at the Cambridge Crystallographic Data Centre with number CCDC 2393186 and can be obtained free of charge via www.ccdc.cam.ac.uk.

Supplementary Materials: The following are available online, Figure S1. ^{1}H NMR of compound **4** in acetone-d_6; Figure S2. COSY (1H–1H 2D NMR) of compound **4** in acetone-d_6; Figure S3. ^{13}C NMR of compound **4** in acetone-d_6; Figure S4. Stacking of ^{13}C NMR + DEPT135 of compound **4**; Figure S5: Low-resolution mass spectra of compound **4**; Figure S6: Zoomed-in view of the HRMS spectra of compound **4** (m/z: range 380–480); Figure S7: Formula determination of compound **4** by HRMS; Figure S8. Infrared spectra of compound **4** (ATR).

Author Contributions: Acquisition of X-ray structure (in 2007), P.H.; refinement of the X-ray structure using modern software, CCDC deposit (in 2024), J.F.; experimental synthetic work and NMR interpretation, P.P.; conceptualization, P.P.; methodology, P.H., J.F. and P.P.; validation, P.H., J.F. and P.P.; formal analysis, P.H., J.F. and P.P.; investigation, P.P.; data curation, J.F. and P.P.; writing—original draft preparation, P.P.; writing—review and editing, J.F. and P.P.; visualization, P.P. All authors have read and agreed to the published version of the manuscript.

Funding: This research was funded by the Agence Nationale de la Recherche (ANR) under grant number ANR-06-BLAN-0384–01, "FerVect".

Data Availability Statement: The data are contained within this article and the Supplementary Materials.

Acknowledgments: The authors thank Michèle Salmain for checking this manuscript and Geoffrey Gontard for his advice in XRD structure refinement.

Conflicts of Interest: The authors declare no conflicts of interest. The funders had no role in the design of the study; in the collection, analyses, or interpretation of data; in the writing of the manuscript; or in the decision to publish the results.

References

1. Sijongesonke, P.; Aderibigbe, B.A. Ferrocene-Based Compounds with Antimalaria/Anticancer Activity. *Molecules* **2019**, *24*, 3604. [CrossRef] [PubMed]
2. Biomol, O.; Hottin, A.; Dubar, F.; Steenackers, A.; Delannoy, P. Iminosugar–ferrocene conjugates as potential anticancer agents. *Org. Biomol. Chem.* **2012**, *10*, 5592–5597. [CrossRef]
3. Huang, X.F.; Tang, J.F.; Ji, J.L.; Wang, X.L.; Ruan, B.F. Synthesis, characterization and antitumor activity of novel amide derivatives containing ferrocenyl pyrazol-moiety. *J. Organomet. Chem.* **2012**, *706*, 113–123. [CrossRef]
4. Pedotti, S.; Ussia, M.; Patti, A.; Musso, N.; Barresi, V.; Condorelli, D.F. Synthesis of the ferrocenyl analogue of clotrimazole drug. *J. Organomet. Chem.* **2017**, *830*, 56–61. [CrossRef]
5. Singh, A.; Lumb, I.; Mehra, V.; Kumar, V. Ferrocene-Appended Pharmacophores: An exciting approach for modulating biological potential of organic scaffolds. *Dalton Trans.* **2019**, *48*, 2840–2860. [CrossRef]
6. Jaouen, G.; Vessières, A.; Top, S. Ferrocifen type anti-cancer drugs. *Chem. Soc. Rev.* **2015**, *44*, 8802–8817. [CrossRef]
7. Kowalski, K. Recent developments in the chemistry of ferrocenyl secondary natural product conjugates. *Coord. Chem. Rev.* **2018**, *366*, 91–108. [CrossRef]
8. Wang, R.; Chen, H.; Yan, W.; Zheng, M.; Zhang, T.; Zhang, Y. Ferrocene-containing hybrids as potential anticancer agents: Current developments, mechanisms of action and structure-activity relationships. *Eur. J. Med. Chem.* **2020**, *190*, 112109. [CrossRef]
9. Sharma, B.; Kumar, V. Has Ferrocene Really Delivered Its Role in Accentuating the Bioactivity of Organic Scaffolds? *J. Med. Chem.* **2021**, *64*, 16865–16921. [CrossRef]
10. Yong, J.; Lu, C.; Yang, M.; Wu, X. New Ferrocene Formates Bearing Isoxazole Moieties: Synthesis, Characterization, X-ray Crystallography, and Preliminarily Cytotoxicity against A549, HCT116, and MCF-7 Cell Lines. *Curr. Pharm. Des.* **2022**, *28*, 2835–2841. [CrossRef]
11. Snegur, L.V. Modern Trends in Bio-Organometallic Ferrocene Chemistry. *Inorganics* **2022**, *10*, 226. [CrossRef]

12. Cybulski, M.; Michalak, O.; Buchowicz, W.; Mazur, M. Ansa–Ferrocene Derivatives as Potential Therapeutics. *Molecules* **2024**, *29*, 4903. [CrossRef] [PubMed]
13. Vessières, A.; Top, S.; Pigeon, P.; Hillard, E.A.; Boubeker, L.; Spera, D.; Jaouen, G. Modification of the estrogenic properties of diphenols by the incorporation of ferrocene. Generation of antiproliferative effects in vitro. *J. Med. Chem.* **2005**, *48*, 3937–3940. [CrossRef] [PubMed]
14. Richard, M.-A.; Hamels, D.; Pigeon, P.; Top, S.; Dansette, P.M.; Lee, H.Z.S.; Vessières, A.; Mansuy, D.; Jaouen, G. Oxidative metabolism of ferrocene analogues of Tamoxifen: Characterization and antiproliferative activities of the metabolites. *ChemMedChem* **2015**, *10*, 981–990. [CrossRef] [PubMed]
15. Wang, Y.; Pigeon, P.; Top, S.; McGlinchey, M.J.; Jaouen, G. Organometallic Antitumor Compounds: Ferrocifens as Precursors to Quinone Methides. *Angew. Chem. Ed. Int.* **2015**, *54*, 10230–10233. [CrossRef]
16. Pigeon, P.; Wang, Y.; Top, S.; Najlaoui, F.; Garcia Alvarez, M.; Bignon, J.; McGlinchey, M.J.; Jaouen, G. A new series of succinimido ferrociphenols and related heterocyclic species induce strong antiproliferative effects, especially against ovarian cancer cells resistant to cisplatin. *J. Med. Chem.* **2017**, *60*, 8358–8368. [CrossRef]
17. Wang, Y.; Richard, M.A.; Top, S.; Dansette, P.M.; Pigeon, P.; Vessières, A.; Mansuy, D.; Jaouen, G. Ferrocenyl quinone methide−thiol adducts as new antiproliferative agents: Synthesis, metabolic formation from ferrociphenols, and oxidative transformation. *Angew. Chem. Int. Ed.* **2016**, *55*, 10431–10434. [CrossRef]
18. Nikitin, K.; Ortin, Y.; Müller-Bunz, H.; Plamont, M.-A.; Jaouen, G.; Vessières, A.; McGlinchey, M.J. Organometallic SERMs (selective estrogen receptor modulators): Cobaltifens, the (cyclobutadiene)cobalt analogues of hydroxytamoxifen. *J. Organomet. Chem.* **2010**, *695*, 595–608. [CrossRef]
19. Hooft, R.W.W. *COLLECT 1997-2000*; Nonius BV: Delft, The Netherlands, 1998.
20. Duisenberg, A.J.M. Indexing in single-crystal diffractometry with an obstinate list of reflections. *J. Appl. Crystallogr.* **1992**, *25*, 92–96. [CrossRef]
21. Duisenberg, A.J.M.; Kroon-Batenburg, L.M.J.; Schreurs, A.M.M. An intensity evaluation method: EVAL-14. *J. Appl. Crystallogr.* **2003**, *36*, 220–229. [CrossRef]
22. Sheldrick, G.M. SHELXT–Integrated Space-Group and Crystal-Structure Determination. *Acta Crystallogr. A Found. Adv.* **2015**, *71*, 3–8. [CrossRef] [PubMed]
23. Sheldrick, G.M. Crystal Structure Refinement with SHELXL. *Acta Crystallogr. C Struct. Chem.* **2015**, *71*, 3–8. [CrossRef] [PubMed]
24. Dolomanov, O.V.; Bourhis, L.J.; Gildea, R.J.; Howard, J.A.K.; Puschmann, H. OLEX2: A Complete Structure Solution, Refinement and Analysis Program. *J. Appl. Crystallogr.* **2009**, *42*, 339–341. [CrossRef]

SUPPORTING INFORMATION

1,1-Bis(4-hydroxyphenyl)-2-ferrocenylbutane

Forté Jérémy [1], Herson Patrick [1,†] and Pigeon Pascal [1,2,*]

[1] Sorbonne Université, UMR 8232 CNRS, IPCM, 4 Place Jussieu, F-75005, Paris, France; jeremy.forte@sorbonne-universite.fr, pascal.pigeon@sorbonne-universite.fr
[2] PSL, Chimie ParisTech, 11 Rue Pierre et Marie Curie, F-75005, Paris, France; pascal.pigeon@chimieparistech.psl.eu

***** Correspondence: pascal.pigeon@chimieparistech.psl.eu
† P. Herson passed away in October 2017.

Summary

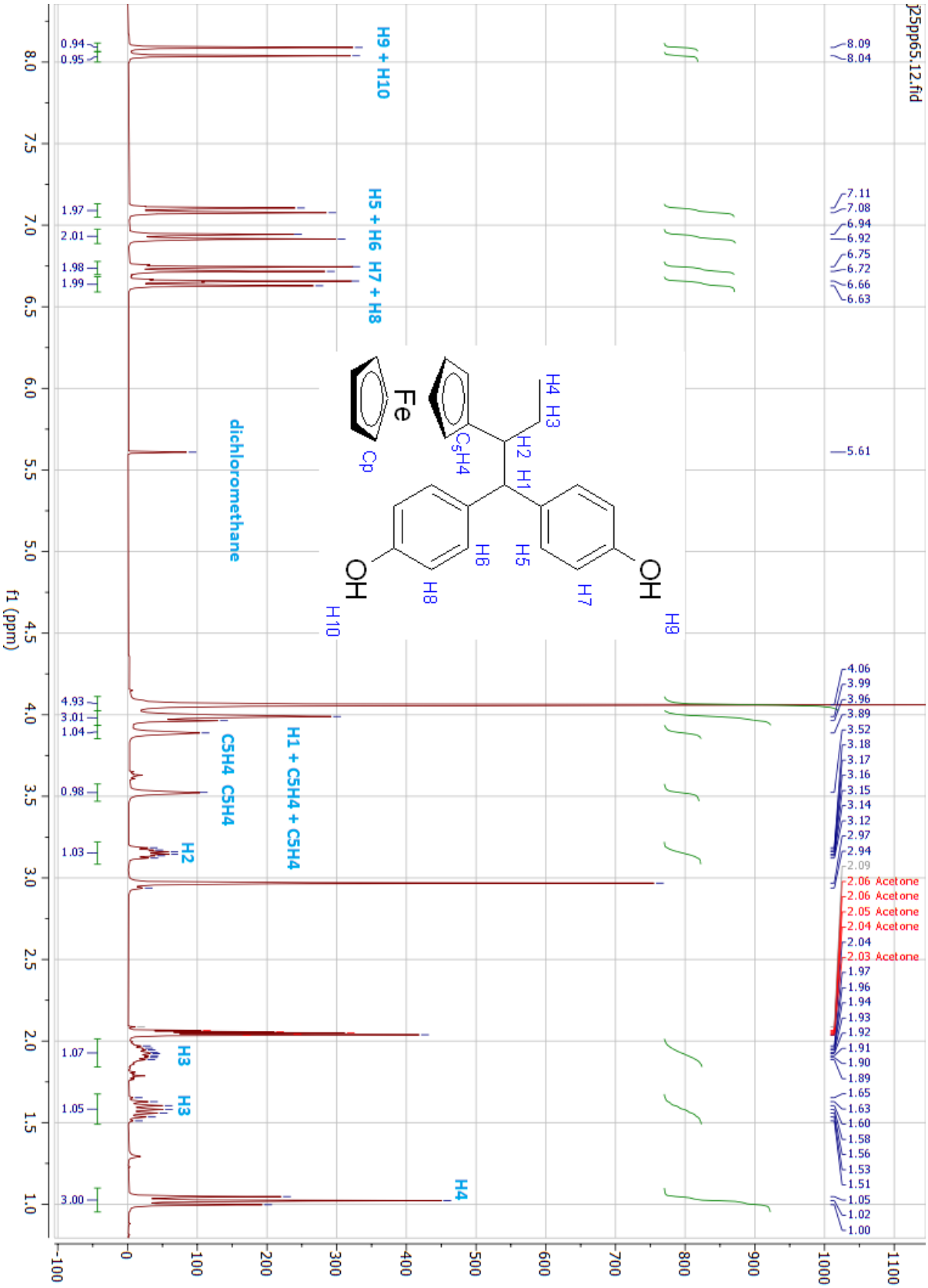

Figure S1. ^{1}H NMR of compound **4** in acetone-d_6

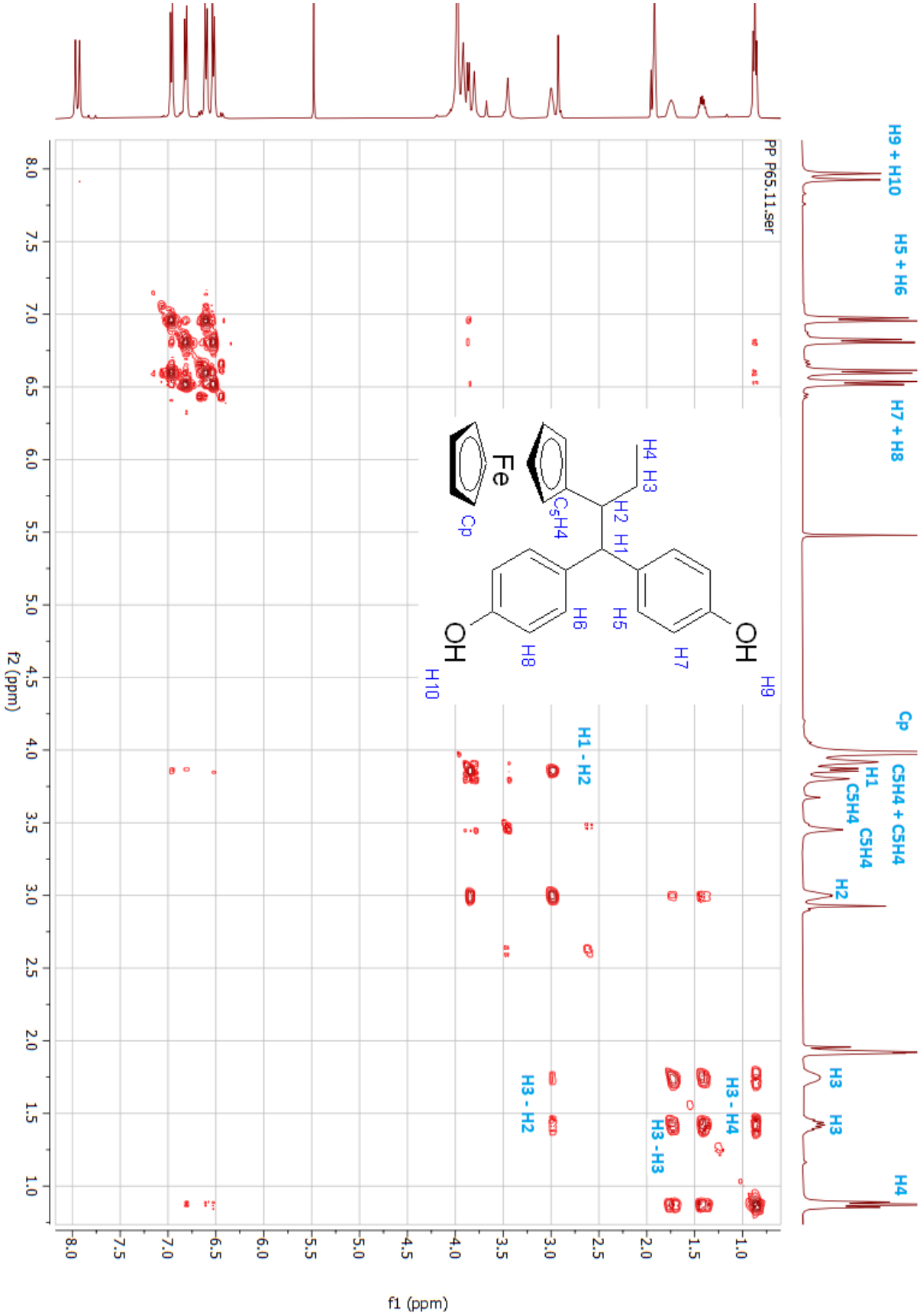

Figure S2. COSY (^{1}H – ^{1}H 2D NMR) of compound **4** in acetone-d_6

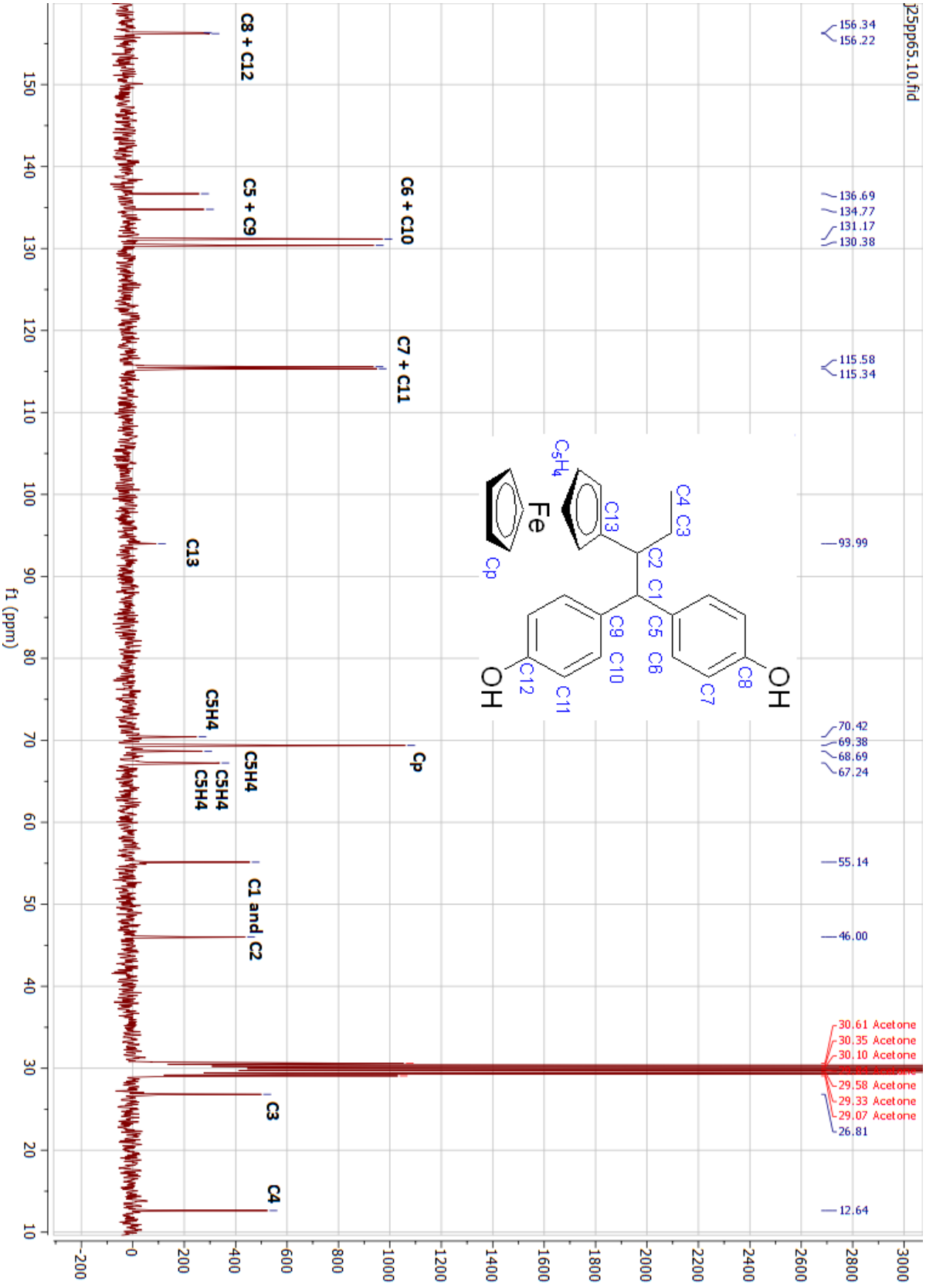

Figure S3. ^{13}C NMR of compound **4** in acetone-d_6

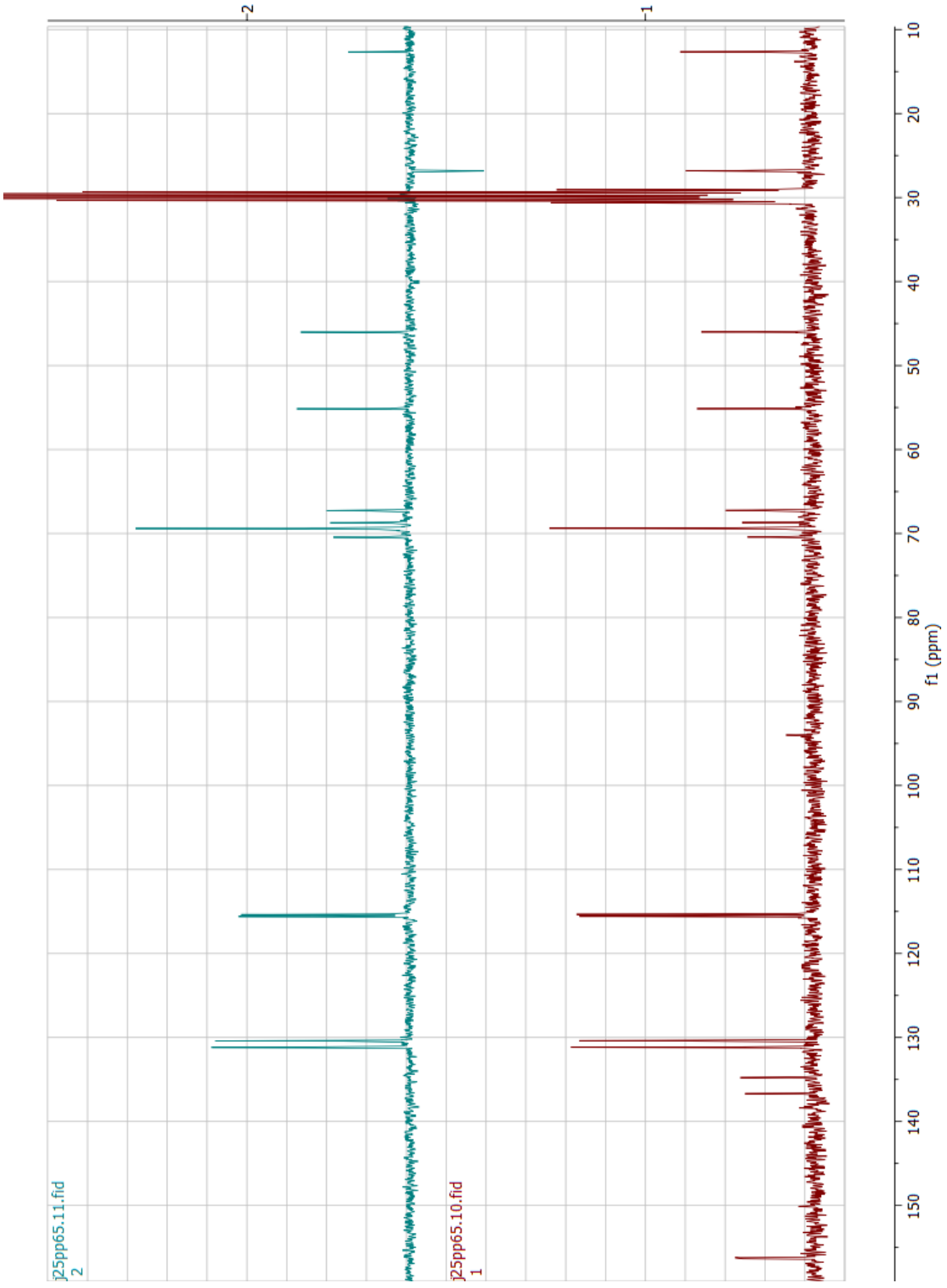

Figure S4. Stacking of ^{13}C NMR + DEPT135 of compound **4**

- CH_2 at 26.8 ppm became negative
- Quaternary carbon atoms disappeared (94.0, 134.8, 136.7, 156.2 and 156.3 ppm)
- CH_3 and CH remained positive

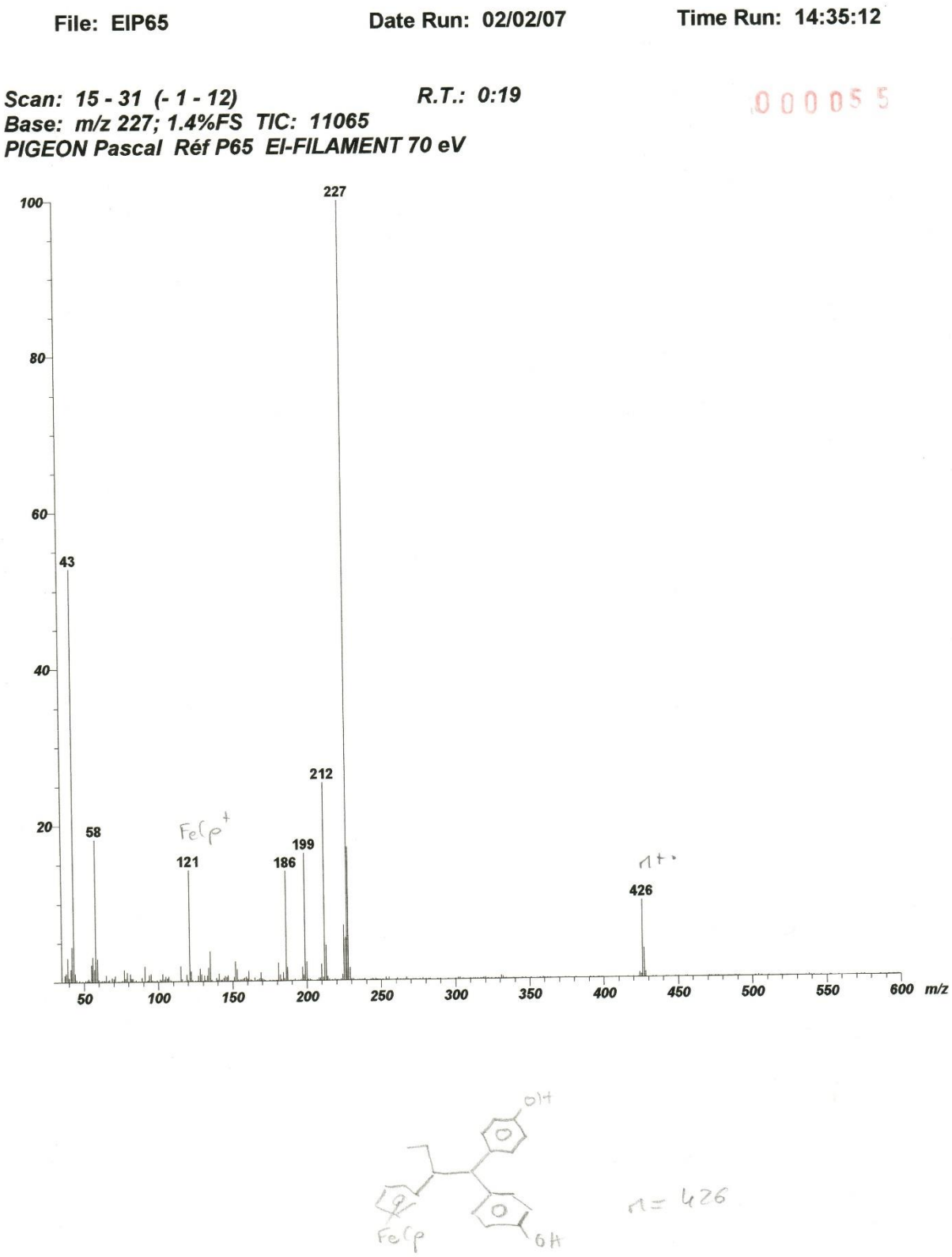

Figure S5. Low resolution mass spectra of compound **4**

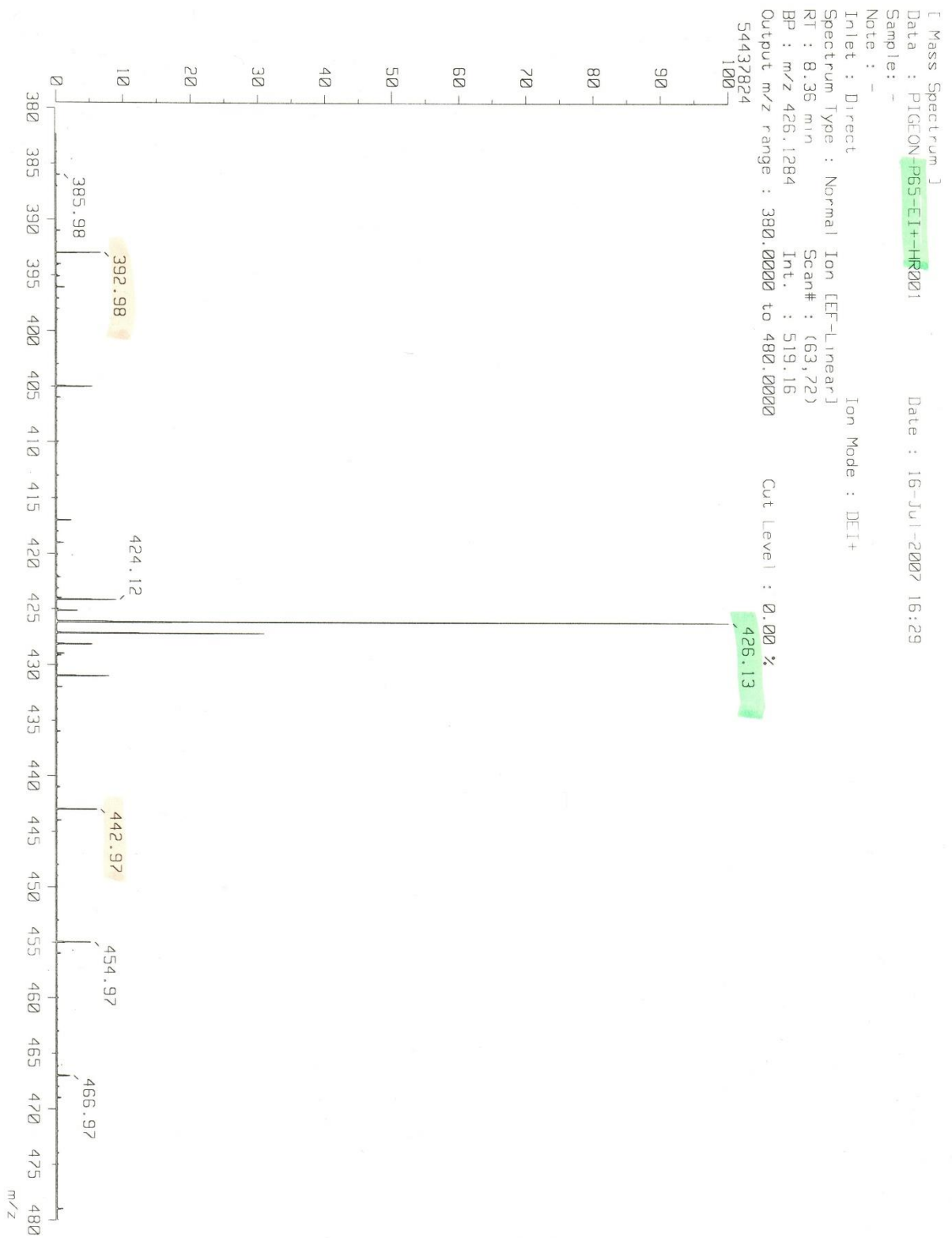

Figure S6. Zoom-in view of the HRMS spectra of compound **4** (m/z: range 380 - 480)

[Elemental Composition] Page: 1
Data : PIGEON-P65-EI+-HR001 Date : 16-Jul-2007 16:29
Sample: -
Note : -
Inlet : Direct Ion Mode : DEI+
RT : 8.36 min Scan#: (63,72)
Elements : C 30/20, H 35/20, O 2/2, Fe 1/1
Mass Tolerance : 10ppm, 10mmu if m/z < 1000, 20mmu if m/z > 2000
Unsaturation (U.S.) : -0.5 - 20.0

Observed m/z	Int%	Err[ppm / mmu]	U.S.	Composition
426.1284	100.0	+0.5 / +0.2	14.5	C 26 H 26 O 2 Fe
427.1322	30.9	-9.0 / -3.8	14.0	C 26 H 27 O 2 Fe

[Theoretical Ion Distribution] Page: 1
Molecular Formula : C26 H26 O2 Fe
(m/z 426.1282, MW 426.3382, U.S. 14.5)
Base Peak : 426.1283, Averaged MW : 426.3398(a), 426.3411(w)

m/z	INT.	
424.1329	6.3054	****
425.1363	1.8528	*
426.1283	100.0000	**********
427.1314	31.7228	**********
428.1340	5.5540	***
429.1364	0.6917	
430.1387	0.0672	
431.1411	0.0053	
432.1435	0.0004	

Figure S7. Formula determination of compound **4** by HRMS

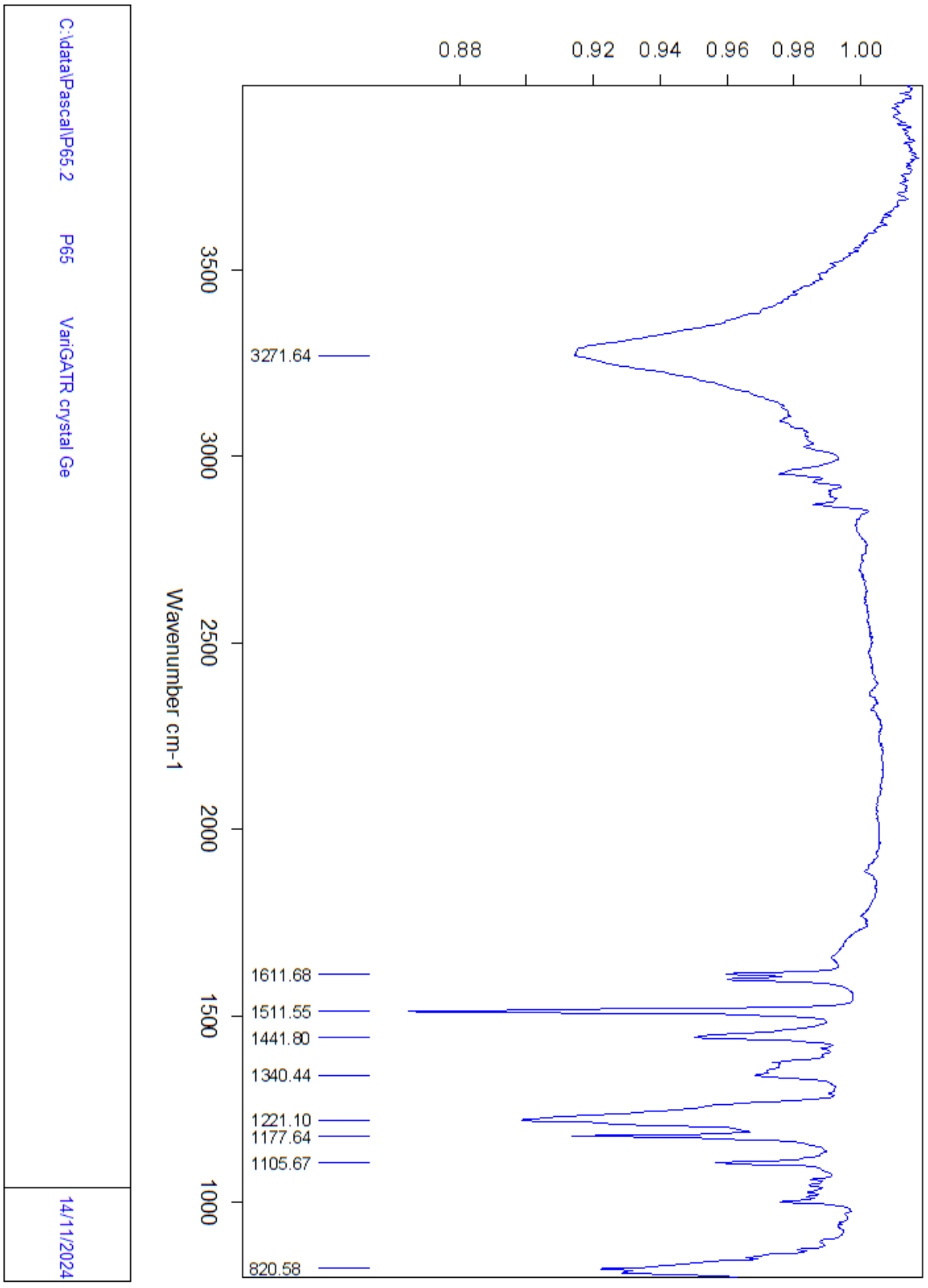

Figure S8. Infrared spectra of compound **4** (ATR)